X-RAY SPECTROMETRY
X-Ray Spectrom. 2005; **34**: 124–127
Published online 20 December 2004 in Wiley InterScience (www.interscience.wiley.com). DOI: 10.1002/xrs.772

Determination of L-shell intensity ratios for Yb, Hf and Ta by a parameter refinement method

A. Carreras,[1]* J. Trincavelli,[1†] R. Bonetto[2†] and G. Castellano[1]

[1] Facultad de Matemática, Astronomía y Física, Universidad Nacional de Córdoba. Ciudad Universitaria, 5000 Córdoba, Argentina
[2] Centro de Investigación y Desarrollo en Ciencias Aplicadas Dr. Jorge Ronco, CONICET — UNLP, Calle 47, No. 257 — Cc 59, 1900 La Plata, Argentina

Received 16 December 2002; Accepted 16 December 2003

Transition rates for radiative decays to the L-shell were obtained for Yb, Hf and Ta by means of a method of experimental and atomic parameter refinement in x-ray fluorescence. An analytical function accounts for continuum and characteristic radiation detection artifacts are also included in the spectral description. The procedure of parameter refinement consists of minimizing quadratic differences between the experimental and predicted spectra through the optimization of the parameters involved in the analytical expression used. Spectra were acquired in an energy-dispersive system with synchrotron monochromatic beams. The results obtained for the sought transition rates are in agreement with the scarce values found in the literature. Copyright © 2004 John Wiley & Sons, Ltd.

INTRODUCTION

Relative intensities of characteristic x-ray lines are essential factors in non-destructive standardless analysis, since in absolute techniques the atomic parameters are not cancelled out by means of intensity ratios. Therefore, an accurate knowledge of these quantities is required in order to perform precise characterization of samples. In the field of atomic physics, relative intensities are associated with the radiative transition rates from the different occupied atomic states, and accurate values for them may be used in testing theoretical models for atomic structure descriptions.

Several studies on the L-shell have been devoted to theoretical prediction,[1] tabulation[2] and experimental determination[3] of intensity ratios involving L-subshells, but some discrepancies exist owing to the experimental uncertainties and to the approximations assumed in the calculations. In the experimental determinations, spectral deconvolution is one of the main problems that arise when determining these parameters owing to the strong peak overlapping in energy-dispersive system L-spectra. Good statistics are not sufficient for this purpose and a careful fitting method is required in order to obtain accurate values for the peak areas. Conventional fitting programs have not shown good performance, but the method of parameter optimization previously developed for electron probe microanalysis[4,5] and x-ray fluorescence (XRF) K-lines[6] appears to be an adequate tool for succeeding in XRF L-line spectrum fitting. In the present work, this method was used for determining relative intensities for Yb, Hf and Ta from synchrotron radiation XRF experiments. A detailed description of the refinement procedure was presented in the original papers, and consists in minimizing the differences between experimental and predicted spectra by optimizing atomic and experimental parameters involved in the analytical expressions used in the predictions. Thus, the quantity to be minimized is

$$\chi^2(\boldsymbol{p}) = \frac{1}{N - N_p} \sum_i \frac{[\widetilde{I}_i(\boldsymbol{p}) - I_i]^2}{I_i}$$

where N is the number of channels in the spectrum, N_p is the number of parameters adjusted, $\widetilde{I}_i(\boldsymbol{p})$ and I_i are respectively the predicted and experimental intensities for the energy E_i of the channel i and $\boldsymbol{p}$ is the vector of parameters to be optimized. A prediction of the spectrum by means of $\widetilde{I}_i(\boldsymbol{p})$ is needed in order to refine $\boldsymbol{p}$ and achieve the set of parameters for the best description of the measured spectrum. Since the expressions involved are complicated functions of the sought parameters, the mentioned minimization must involve a numerical procedure. In the next section, a brief review of the features involved in spectrum prediction and the optimization method is given.

SPECTRUM PREDICTION

Several aspects must be taken into account in order to obtain a complete description of the measured spectra, that is, the background and characteristic line contributions and detection artifacts.

In the applications presented here, the background continuum below the characteristic peaks was always negligible, owing to the use of monochromatic incident beams and the low scattering achieved in the vacuum

*Correspondence to: A. Carreras, Facultad de Matemática, Astronomía y Física, Universidad Nacional de Córdoba, Ciudad Universitaria, 5000 Córdoba, Argentina.
E-mail: alejo@quechua.fis.uncor.edu
†Consejo Nacional de Investigaciones Científicas y Técnicas de la República Argentina..
Contract/grant sponsor: Consejo Nacional de Investigaciones Científicas y Técnicas.
Contract/grant sponsor: Secretaría de Ciencia y Técnica (Universidad de Córdoba).
Contract/grant sponsor: Agencia Córdoba Ciencia SE.

chamber of the sample. Therefore, a constant value B was sufficient when accounting for its contribution. In a more general case, a function for the background $B(E_i)$ may be required.

Expressions arising from fundamental parameters were used in order to calculate characteristic intensities.[7] This means that the intensity $P_{j,q}$ of the line q from the element j can be written as

$$P_{j,q} = \alpha C_j \frac{N_A \tau_j(E_0)}{A_j} \omega_j f_{j,q} \times \frac{1 - \exp\{-[\mu(E_0)\csc\psi_1 + \mu(E_{j,q})\csc\psi_2]t\}}{\mu(E_0)\csc\psi_1 + \mu(E_{j,q})\csc\psi_2} \varepsilon_{j,q} \frac{\Delta\Omega}{4\pi} \quad (1)$$

where t is the mass thickness of the sample, E_0 is the incident photon energy, α depends on the L-subshell involved and is proportional to the number of incident photons, C_j is the mass concentration of element j, A_j its atomic weight, N_A is Avogadro's number, $\tau_j(E_0)$ is the photoelectric cross-section of element j for E_0, ω_j is the fluorescence yield for the atomic shell considered, $f_{j,q}$ is the radiative transition rate corresponding to the line q from the element j normalized to the total emission from the atomic subshell, $\mu(E_0)$ and $\mu(E_{j,q})$ are the mass absorption coefficients of the sample for the incident and the characteristic energy, respectively, ψ_1 and ψ_2 are the incident and take-off angles, $\varepsilon_{j,q}$ is the detector efficiency for the corresponding energy and $\Delta\Omega$ is the solid angle subtended by the detector. This expression does not account for multiple scattering effects, as they are negligible in the samples analyzed.

Concerning detection features, spectrum acquisition was performed by means of a silicon detector, involving a proportional conversion of the incident photons into an electrical pulse. This pulse is registered in a multichannel analyzer, for which two parameters must be supplied for a linear calibration of energies: the 'gain' and the 'zero'. Both parameters may be used with variable values in the spectral prediction.

Statistical fluctuations in the initial number of excitations produced by arriving photons and electronic noise of the amplification process cause a broadened peak when detecting a single line of a given energy. To a first approximation, a characteristic line of photons with energy $E_{j,q}$ produces a peak of intensity $P_{j,q}$ [see Eqn (1)] with Gaussian distribution

$$G_{j,q}(E_i) = \frac{1}{\sqrt{2\pi}\sigma_{j,q}} \exp\left[-\frac{(E_i - E_{j,q})^2}{2\sigma_{j,q}^2}\right]$$

In this equation, the standard deviation is a function of the photon energy given by

$$\sigma_{j,q} = (n^2 + \varepsilon F E_{j,q})^{1/2} \quad (2)$$

where n is the uncertainty due to the electronic noise, F is the Fano factor and E is the mean energy required for a single electron–hole pair formation (3.76 eV at 77 K). However, a correction of this Gaussian shape is required in order to account for another feature of the detection process. If some of the charge carriers produced by a photon arriving at the detector are 'trapped' before being collected, the output sent to the amplifier will correspond to an energy lower than the original one. This effect is manifested by low-energy tails in asymmetric peaks. More asymmetric peaks are observed for soft x-ray lines, for which the absorption occurs near the detector surface, between the active volume and the dead layer, where a higher probability of trapping is expected. In order to account for this, a modification to the Gaussian function is introduced by means of the Hypermet[8] function

$$H_{j,q}(E_i) = A[G_{j,q}(E_i) + S_{j,q}(E_i) + T_{j,q}(E_i)]$$

in which A is a normalization factor, $S_{j,q}(E_i)$ is the step function of height $s_{j,q}$ convoluted by the Gaussian:

$$S_{j,q}(E_i) = s_{j,q}\mathrm{erfc}\left(\frac{E_i - E_{j,q}}{\sqrt{2}\sigma_{j,q}}\right)$$

and $T_{j,q}(E_i)$ is an exponential tail of width $\beta_{j,q}$ and height $t_{j,q}$ convoluted by the Gaussian:

$$T_{j,q}(E_i) = t_{j,q} e^{(E_i - E_{j,q})/\beta_{j,q}} \mathrm{erfc}\left(\frac{E_i - E_{j,q}}{\sqrt{2}\sigma_{j,q}} + \frac{\sigma_{j,q}}{\sqrt{2}\beta_{j,q}}\right)$$

The parameters $s_{j,q}$, $t_{j,q}$ and $\beta_{j,q}$ of these functions characterize the shape of peaks, and they are not known *a priori*. In order to take into account peak asymmetries, they must be refined starting from some rough initial estimation.

There still remain some artifacts that have not been considered in this application, since they would not influence the results, namely 'escape' and 'sum' peaks, and the spurious peak that may appear at 1.739 keV due to the internal fluorescent Si peak. However, in other applications these effects can be easily incorporated.

With all these details in mind, the total intensity for channel i is

$$\tilde{I}_i(\boldsymbol{p}) = B + \sum_{j,q} P_{j,q} H_{j,q}(E_i) \quad (3)$$

in which the constant background intensity B is added to the contribution of the characteristic lines $P_{j,q}$ spread by the Hypermet function $H_{j,q}(E_i)$. The components of vector $\boldsymbol{p}$, implicit in the right-hand side of the Eqn (3), are the parameters that can be optimized, namely the background B and the scaling factor α for peaks of Eqn (1); the gain and zero of the detection chain; the peak width factors n and F of Eqn (2); the transition rates $f_{j,q}$; the fluorescence yields ω_j and the mass concentrations C_j of Eqn (1); the parameters involved in the function $H_{j,q}$ for each peak; the four thicknesses associated with the detector efficiency; the transition energies for the involved decays; etc.

Since χ^2 involves the parameters to be refined in a very complicated way, a robust minimization procedure is required in addition to a careful strategy for the parameter-space exploration, in order to prevent falling in local minima. The downhill simplex algorithm[9] was chosen for this purpose, since it involves only function evaluations and avoids numerical derivatives, which produce strong truncation errors that often interfere with reaching the global minimum.

Once convergence is achieved, uncertainties for the parameters considered are assessed. To this end, the selected spectral region is regarded as a vector $\boldsymbol{y}$ which contains the number of counts in each channel. The optimized parameters also conform a vector $\boldsymbol{p}$, and the function relating both vectors is a matrix $M(\boldsymbol{p})$. The uncertainties of the parameters p_i, arising from the variance–covariance matrix V_p can therefore be related to the variance–covariance matrix V_y for the experimental spectrum by means of[10]

$$V_p = [A^T (V_y)^{-1} A]^{-1}$$

where $A_{ij} = \partial M_i / \partial p_j$. These derivatives are calculated numerically in order to yield the matrix V_p, whose diagonal elements are the searched variances for the parameters p_i.

With this procedure, statistical errors for each spectral channel were propagated over the parameters refined (relative transition rates). Additional uncertainty sources such as geometric factors, photon beam energy, etc., were neglected. The influence of these experimental errors is very weak, as the corresponding matrix corrections are cancelled out (to a first approximation) when normalizing each group of lines, since they have close energies.

In the applications shown here, pure samples were used, so no concentration refinement was necessary. Characteristic energies were taken from Bearden[11] and mass absorption coefficients from Heinrich.[12] In all the optimizations carried out, the factor $\alpha\omega_j(N_A/A_j)\Delta\Omega/(4\pi)$ was taken as a single parameter for each subshell, whereas transition rates were the main parameters involved in the refinements.

EXPERIMENTAL

Spectra were acquired at the XRF beamline of the Laboratório Nacional de Luz Síncrotron (Campinas, Brazil), in an experimental mount corresponding to conventional 45°–45° geometry. Incident x-ray beams were monochromatized by means of an Si(220) double-crystal monochromator. An Si(Li) detector with a resolution of 168 eV at Mn Kα was used for recording spectra.

In order to reduce absorption in the air, the samples were mounted in a vacuum chamber to 0.2 mbar. Negligible background radiation was consequently achieved, because of the low scattering of the incident and fluorescent x-ray beams. The contribution of multiple scattering events was not important owing to the sample thicknesses chosen. However, the measured intensities were corrected for absorption effects of both incident and characteristic radiation. Experimental conditions for the different measurements are shown in Table 1.

Table 1. Experimental conditions for the different samples measured

Z	Element	E_0 (keV)	Thickness (cm)
70	Yb	11.0	0.0100
72	Hf	14.0	0.0254
73	Ta	15.0	0.0127

On the other hand, since the detector was outside the chamber, a sealing window of kapton must be traversed by the characteristic x-rays before reaching the detector. The correction accounting for the effect of absorption in this window was never negligible for the energies of the lines considered.

RESULTS AND DISCUSSION

The fitting of a particular spectrum requires several minimization steps, refining a different set of parameters each time. The way to choose the best set of parameters for every step represents a cautious task that will define the risk of falling in local minima. If the strategy followed is appropriate, convergence is reached with quite adequate predictions even for complicated spectra. Figure 1 shows the final fitting for an Hf spectrum corresponding to 14 keV photon beams.

L-shell transition rates obtained for Yb, Hf and Ta are compared with theoretical and experimental values given by other workers in Tables 2–4. Good agreement was achieved in spite of the inherent limitations of an EDS set-up related to the severe overlapping of some characteristic peaks. The discrepancies with data from other workers are generally of the same order as the already existing differences. Results

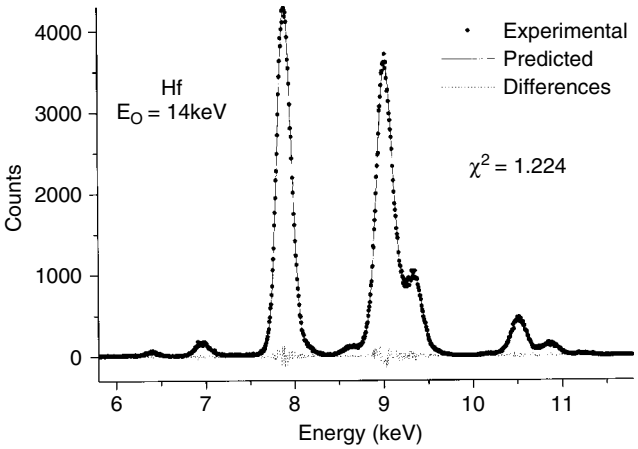

Figure 1. Hafnium spectrum predicted by the present method.

Table 2. Transition rates for the Yb L-shell

Transition		This work	CRC[3]	Perkins *et al*.[2]
α_1	L_3M_5	0.729 ± 0.010	0.7322	0.7196
α_2	L_3M_4	0.0711 ± 0.0091	0.0817	0.0815
$\beta_{2,15}$	$L_3N_{4,5}$	0.1549 ± 0.0015	0.1420	0.1366
ℓ	L_3M_1	0.03393 ± 0.00093	0.0327	0.0511
β_6	L_3N_1	0.0107 ± 0.0011	0.0086	0.0084
β_1	L_2M_4	0.8095 ± 0.0033	0.8251	0.8213
γ_1	L_2N_4	0.1474 ± 0.0024	0.1499	0.1463
η	L_2M_1	0.0295 ± 0.0038	0.0174	0.0247
γ_5	L_2N_1	0.0078 ± 0.0024		0.0055
γ_8	L_2O_1	0.0057 ± 0.0021		0.0010
β_3	L_1M_3	0.489 ± 0.012	0.4337	0.4282
β_4	L_1M_2	0.263 ± 0.014	0.2840	0.3231
γ_3	L_1N_3	0.1213 ± 0.0068	0.1293	0.1078
γ_4	$L_1O_{2,3}$	0.0195 ± 0.0015		0.0236

Table 3. Transition rates for the Hf L-shell

Transition		This work	CRC[3]	Perkins *et al.*[2]
α_1	L_3M_5	0.728 ± 0.012	0.7194	0.7178
α_2	L_3M_4	0.070 ± 0.011	0.0803	0.0813
$\beta_{2,15}$	$L_3N_{4,5}$	0.1583 ± 0.0013	0.1534	0.1387
ℓ	L_3M_1	0.03158 ± 0.00074	0.0330	0.0492
$\beta_{5,7}$	$L_3O_{4,5}$	0.00400 ± 0.00051		0.00313
β_1	L_2M_4	0.8062 ± 0.0026	0.8221	0.8181
γ_1	L_2N_4	0.1571 ± 0.0017	0.1515	0.1488
η	L_2M_1	0.0274 ± 0.0027	0.0171	0.0238
γ_5	L_2N_1	0.0074 ± 0.0019		0.0055
γ_6	L_2O_4	0.00180 ± 0.00056		0.0016
β_3	L_1M_3	0.4038 ± 0.0088	0.4237	0.4193
β_4	L_1M_2	0.313 ± 0.010	0.2872	0.3253
γ_3	L_1N_3	0.106 ± 0.040	0.1300	0.1072
γ_2	L_1N_2	0.112 ± 0.045	0.0989	0.0789
γ_4	$L_1O_{2,3}$	0.0274 ± 0.0018		0.0261

Table 4. Transition rates for the Ta L-shell

Transition		This work	Scofield[1]	Perkins *et al.*[2]
α_1	L_3M_5	0.696 ± 0.017	0.7175	0.7164
α_2	L_3M_4	0.092 ± 0.016	0.0815	0.0812
$\beta_{2,15}$	$L_3N_{4,5}$	0.1589 ± 0.0015	0.1489	0.1398
ℓ	L_3M_1	0.03136 ± 0.00076	0.0370	0.0483
β_6	L_3N_1	0.0160 ± 0.0029	0.0089	0.0088
β_7	L_3O_1	0.00176 ± 0.00052		0.0018
β_1	L_2M_4	0.8029 ± 0.0027	0.8087	0.8159
γ_1	L_2N_4	0.1620 ± 0.0027	0.1582	0.1501
η	L_2M_1	0.0274 ± 0.0032	0.0233	0.0234
γ_5	L_2N_1	0.0071 ± 0.0028	0.0055	0.0055
γ_6	L_2O_4	0.00051 ± 0.00023	0.0036	0.0028
β_3	L_1M_3	0.4096 ± 0.0081	0.4123	0.4127
β_4	L_1M_2	0.3059 ± 0.0098	0.3228	0.3263
γ_3	L_1N_3	0.093 ± 0.017	0.1096	0.1069
γ_2	L_1N_2	0.131 ± 0.023	0.0807	0.0797

with uncertainties >50% were omitted from the tables, because they correspond to very weak lines, which should be determined with a spectrometer of better resolution.

CONCLUSION

L-shell transition rates for Yb, Hf and Ta were determined by means of a previously developed parameter optimization method. This method has proved to be an adequate tool for fitting L-spectra of heavy elements, with the consequent determination of relative peak intensities, although for the appropriate determination of less intense lines certain inconveniences remain.

The program developed showed good performance for a number of lines in each studied element, which represent ~99% of the intensity emitted from the corresponding atoms. It is worth emphasizing that in these examples, conventional fitting programs were inadequate. In the near future, other heavy elements for which experimental L transition rates are practically non-existent will be studied.

Acknowledgements

The authors acknowledge financial support from the Consejo Nacional de Investigaciones Científicas y Técnicas (Argentina), the Secretaría de Ciencia y Técnica (Universidad Nacional de Córdoba) and the Agencia Córdoba Ciencia SE. This work was partially performed at the LNLS (Brazil) under proposal XRD 614/00.

REFERENCES

1. Scofield J. *Phys. Rev. A* 1974; **10**: 1507.
2. Perkins ST, Cullen DE, Chen MH, Hubbell JH, Rathkopf J, Scofield JH. *Tables and Graphs of Atomic Subshells and Relaxation Data Derived from LLNL Evaluated Atomic Data Library (EADL), $Z = 1$–100*. Report UCRL-50400, vol. 30. Lawrence Livermore National Laboratory: Livermore, CA, 1991.
3. Lide DR (ed). *Handbook of Chemistry and Physics* (74th edn). CRC Press: Boca Raton, FL, 1994.
4. Bonetto R, Castellano G, Trincavelli J. *X-Ray Spectrom.* 2001; **30**: 313.
5. Trincavelli J, Castellano G, Bonetto R. *Spectrochim. Acta Part B* 2002; **57**: 919.
6. Carreras A, Bonetto R, Stutz G, Trincavelli J, Castellano G. *X-Ray Spectrom.* 2002; **31**: 173.
7. Sherman J. *Spectrochim. Acta* 1955; **7**: 283.
8. Phillips G, Marlow K. *Nucl. Instrum. Methods* 1976; **137**: 525.
9. Nelder J, Mead R. *Comput. J.* 1965; **7**: 308.
10. Young R. *The Rietveld Method*. International Union of Crystallography, Oxford University Press: Oxford, 1993.
11. Bearden JA. *Rev. Mod. Phys.* 1967; **39**: 78.
12. Heinrich K. In *X-Ray Optics and Microanalysis*, Brown J, Packwood R (eds). University of Western Ontario: Ontario, 1987; 67.